

## REFERENCES

- [1] J. Ward, "Space-time adaptive processing for airborne radar," Lincoln Laboratory, Massachusetts Inst. of Technol. (MIT), Cambridge, MA, Tech. Rep. 1015, 1994.
- [2] F. C. Robey, D. R. Fuhrmann, E. J. Kelly, and R. Nitzberg, "A CFAR adaptive matched filter detector," *IEEE Trans. Aerosp. Electron. Syst.*, vol. 28, no. 1, pp. 208–216, Jan. 1992.
- [3] A. Haimovich, "The eigencanceler: Adaptive radar by eigenanalysis methods," *IEEE Trans. Aerosp. Electron. Syst.*, vol. 32, no. 2, pp. 532–542, Apr. 1996.
- [4] I. P. Kirsteins and D. W. Tufts, "Adaptive detection using low rank approximation to a data matrix," *IEEE Trans. Aerosp. Electron. Syst.*, vol. 30, no. 1, pp. 55–67, Jan. 1994.
- [5] J. S. Goldstein and I. S. Reed, "Reduced-rank adaptive filtering," *IEEE Trans. Signal Process.*, vol. 45, no. 2, pp. 492–496, Feb. 1997.
- [6] J. S. Goldstein, I. S. Reed, and L. L. Scharf, "A multistage representation of the Wiener filter based on orthogonal projections," *IEEE Trans. Inf. Theory*, vol. 44, no. 7, pp. 2943–2959, Nov. 1998.
- [7] G. H. Golub and C. F. Van Loan, *Matrix Computations*, 3rd ed. Baltimore, MD: The Johns Hopkins Univ. Press, 1996.
- [8] P. S. Chang and A. N. Wilson, Jr, "Analysis of conjugate gradient algorithms for adaptive filtering," *IEEE Trans. Signal Process.*, vol. 48, no. 2, pp. 409–418, Feb. 2000.
- [9] M. E. Weippert, J. D. Hiemstra, J. S. Goldstein, and M. D. Zoltowski, "Insights from the relationship between the multistage Wiener filter and the method of conjugate gradients," in *Proc. Sensor Array Multichannel Signal Process. Workshop*, Rosslyn, VA, Aug. 2002, pp. 388–392.
- [10] L. L. Scharf, E. K. P. Chong, M. D. Zoltowski, J. S. Goldstein, and I. S. Reed, "Subspace expansion and the equivalence of conjugate direction and multistage wiener filters," *IEEE Trans. Signal Process.*, vol. 56, no. 10, pp. 5013–5019, Oct. 2008.
- [11] C. Jiang, H. Li, and M. Rangaswamy, "Conjugate gradient parametric detection of multichannel signals," *IEEE Trans. Aerosp. Electron. Syst.*, vol. 48, no. 1, Apr. 2012.
- [12] I. R. Kirsteins and H. Ge, "Performance analysis of Krylov space adaptive beamformers," in *Proc. 4th IEEE Workshop Sensor Array Multichannel Process. (SAM)*, Waltham, MA, Jul. 2006, pp. 16–20.
- [13] B. D. Van Veen and K. M. Buckley, "Beamforming: A versatile approach to spatial filtering," *IEEE Signal Process. Mag.*, pp. 4–24, Apr. 1988.
- [14] L. E. Brennan and I. S. Reed, "Theory of adaptive radar," *IEEE Trans. Aerosp. Electron. Syst.*, vol. AES-9, no. 2, pp. 237–252, 1973.
- [15] M. Rangaswamy, F. C. Lin, and K. R. Gerlach, "Robust adaptive signal processing methods for heterogeneous radar clutter scenarios," *Signal Process.*, vol. 84, no. 9, pp. 1477–1733, Sep. 2004.
- [16] J. S. Bergin and P. M. Techau, "High-Fidelity Site-Specific Radar Simulation: KASSPER'02 Workshop Datacube," Information Syst. Laboratories, Inc., Vienna, VA, Tech. Rep. ISL-SCRD-TR-02-105, 2002.

## Inverse Methods for Reconstruction of Channel Taps in OFDM Systems

Tomasz Hrycak, Saptarshi Das, and Gerald Matz

**Abstract**—We describe a novel pilot-aided method for estimation of doubly selective wireless channels in OFDM systems. We compute the first few Fourier coefficients of each channel tap from the pilot information. We then estimate the BEM coefficients of the channel taps from their respective Fourier coefficients using a recently developed inverse reconstruction method. For a system with  $L$  channel taps, the proposed method uses  $\mathcal{O}(L \log L)$  operations and  $\mathcal{O}(L)$  memory per OFDM symbol.

We validate our method by simulating a system conforming to the IEEE 802.16e standard.

**Index Terms**—Basis Expansion Model (BEM), channel estimation, doubly selective, inverse reconstruction method, OFDM.

### I. INTRODUCTION

#### A. Motivation

Orthogonal frequency-division multiplexing (OFDM) is a multicarrier modulation technique with several advantages, e.g., high spectral efficiency and robustness against multipath propagation. OFDM based communications through rapidly varying doubly selective wireless channels attract a great deal of scientific and commercial interest. OFDM is used in high-mobility communication systems, e.g., Mobile WiMAX (IEEE 802.16e), WAVE (IEEE 802.11p), and DVB-T (ETSI EN 300 744).

Communication systems using multicarrier modulation schemes over doubly selective channels are affected by intercarrier interference (ICI), which makes equalization more difficult. ICI is caused by the Doppler effect, and the carrier frequency offset. The Doppler effect is proportional to the receiver velocity and the carrier frequency and depends inversely on the intercarrier frequency offset.

In the case of scalable OFDM, the required bandwidth grows with the number of subcarriers. Increasing the bandwidth increases the sampling frequency, which in turn proportionally increases the number of resolvable discrete multipaths. For example, Mobile WiMAX with  $K$  subcarriers typically exhibits a discrete path delay of  $\frac{K}{8}$ ; see [1]. A large number of channel taps makes channel estimation much harder. Such challenging regimes require an accurate channel estimation algorithm, whose complexity scales with the number of subcarriers.

#### B. Previous Work

Doubly selective channels, whose taps vary with time, are commonly estimated using the Basis Expansion Model (BEM); see [2] and [3]. The BEM approximates the channel taps by linear combinations of prescribed basis functions. In this approach, channel estimation reduces to estimation of the basis coefficients of the channel taps. Several bases have been proposed for modeling doubly selective channels. The BEM with complex exponentials (CE-BEM) [4] gives rise to a banded

---

Manuscript received August 02, 2011; revised November 18, 2011; accepted January 11, 2012. Date of publication February 10, 2012; date of current version April 13, 2012. The associate editor coordinating the review of this manuscript and approving it for publication was Prof. Lieven De Lathauwer. This paper was supported by the FWF Grant S10602-N13.

T. Hrycak and S. Das are with the Faculty of Mathematics, University of Vienna, Vienna, Austria (e-mail: saptarshi.das@univie.ac.at).

G. Matz is with Institut für Nachrichtentechnik und Hochfrequenztechnik, Vienna University of Technology, Vienna, Austria.

Digital Object Identifier 10.1109/TSP.2012.2187522

frequency-domain channel matrix. Unfortunately, the CE-BEM is not sufficiently accurate for doubly selective channels due to the Gibbs phenomenon; see [2]. Other BEMs include the generalized CE-BEM (GCE-BEM) [5], the polynomial BEM (P-BEM) [6], [7], and the BEM with discrete prolate spheroidal sequences (DPSSs) [2].

The papers [3] and [7] are focused on estimation in extreme regimes, where the channel taps noticeably fluctuate within a single OFDM symbol duration. For a channel with  $L$  taps, the method presented in [3] requires  $\mathcal{O}(L^2)$  flops and memory to estimate the BEM coefficients. The method of [7] requires only  $\mathcal{O}(L \log L)$  operations and  $\mathcal{O}(L)$  memory for the same task.

Typically, equalization of the received signal is done after estimation of the channel. A method proposed in [8] uses the estimated BEM coefficients directly for equalization of the received signal, without ever creating the channel matrix. With  $K$  OFDM subcarriers, that equalizer has a complexity of  $\mathcal{O}(K \log K)$  and requires  $\mathcal{O}(K)$  memory. There exist other low-complexity equalization methods, e.g., [9] and [10].

### C. Contributions

In [7], the authors present a pilot-aided method for computation of the Fourier coefficients of the channel taps, which requires  $\mathcal{O}(L \log L)$  operations and  $\mathcal{O}(L)$  memory. Subsequently, the BEM coefficients in a fixed, but arbitrary basis, are computed from the Fourier coefficients of the taps by the orthogonal projection on the subspace spanned by the basis. In this paper, we are only concerned with estimation of the BEM coefficients from the estimated Fourier coefficients. Specifically, we study *the inverse reconstruction method* [11]. While the inverse method can be used with arbitrary bases, we develop our approach using the basis of the prolate spheroidal wave functions (PSWFs); see, e.g., [12]. We estimate the basis coefficients of the taps, however, without necessarily reconstructing the full channel matrix. For equalization, we use the method proposed in [8].

The paper is organized as follows. In Section II, we describe our OFDM transmission model, the basis expansion model of the wireless channel, introduce the PSWF-BEM, and summarize the method of [7] for estimation of the Fourier coefficients of the channel taps. In Section III, we formulate the inverse reconstruction method. In Section IV, we first provide an overview of the BEM coefficients estimation using the inverse method, next we describe further details of the BEM estimation algorithm and its complexity analysis. We present our simulation results in Section V, and our conclusions in Section VI. Our simulations conform to the IEEE 802.16e standard [1].

## II. SYSTEM MODEL

### A. Transmitter–Receiver Model

We consider a single-user CP-OFDM system with  $K$  subcarriers and a cyclic prefix of length  $L_{cp}$ . We denote the transmission bandwidth by  $B$ , and the sampling period by  $T_s = 1/B$ . We assume that  $L_{cp}T_s$  exceeds the channel's maximum path delay and, consequently, no intersymbol interference (ISI) occurs.

The time-domain transmit signal  $x[n]$  is obtained by modulating the frequency-domain transmit symbols  $A[k]$  ( $k = 0, \dots, K-1$ ) using the inverse discrete Fourier transform (IDFT) as follows:

$$x[n] = \frac{1}{\sqrt{K}} \sum_{k=0}^{K-1} A[k] e^{j2\pi \frac{nk}{K}}, \quad n = -L_{cp}, \dots, K-1. \quad (1)$$

We note that the indices  $n = -L_{cp}, \dots, -1$  correspond to the cyclic prefix.

We denote the channel tap with delay  $l$  by  $h_l$ ,  $0 \leq l \leq L-1$ , where  $L$  is maximum discrete-time delay. We assume that  $L = L_{cp}$ . The

values assumed by the taps at the sampling times are denoted by  $h_l[n]$ , i.e.,  $h_l[n] = h_l(nT_s)$ . After discarding the cyclic prefix, the receive signal  $y[n]$  is given by the formula

$$y[n] = \sum_{l=0}^{L-1} h_l[n] x[n-l] + w[n], \quad n = 0, \dots, K-1 \quad (2)$$

where  $w[n]$  denotes complex additive noise.

### B. Basis Expansion Model

In the framework of the Basis Expansion Model (BEM), each channel tap  $h_l$  is represented as a linear combination of the basis functions [2], [3]. The number of basis functions used is called the model order, and denoted by  $M$ . In this paper, we study rapidly varying channels, and analyze the channel taps within a single OFDM symbol duration  $KT_s$  (excluding CP). Consequently, we represent the  $l$ th channel tap as

$$h_l(t) = \sum_{m=0}^{M-1} b_{lm} B_m(t), \quad 0 \leq t \leq KT_s \quad (3)$$

$l = 0, \dots, L-1$ , and  $b_{lm}$  is the  $m$ th basis coefficient of the  $l$ th channel tap.

### C. BEM With Prolate Spheroidal Wave Functions

In [2], the authors view the channel taps as band-limited functions of time, and introduce a BEM with the discrete prolate spheroidal sequences (DPSSs) [13]. Instead of the DPSSs, we use their continuous counterparts, the prolate spheroidal wave functions (PSWFs) [12] as a basis for the wireless channel taps. The resulting BEM is called a PSWF-BEM. Advantages of the PSWF-BEM can be summarized as follows. For a fixed model order  $M$ , the PSWF-BEM approximates the channel taps as continuous functions of time, and the PSWFs depend only on the time–bandwidth parameter [12], which reflects the magnitude of the maximum Doppler shift. In contrast, the DPSSs are defined at discrete time instances. Moreover, the DPSS-BEM depends on the number of samples  $N$ , which is typically equal to the number of subcarriers  $K$ . However, the number of subcarriers is a transmission parameter, which is unrelated to intrinsic properties of the channel. The PSWFs are the limits of the DPSSs as the number of samples  $N$  increases to infinity. In practice, the two approaches result in a similar accuracy of approximation, with the PSWF-BEM being simpler.

Our definition of the PSWFs follows [13, p. 383]. For a fixed parameter  $c > 0$ , we consider the eigenproblem

$$\int_{-1}^1 \frac{\sin c(x-y)}{\pi(x-y)} \psi(y) dy = \lambda \psi(x), \quad -1 \leq x \leq 1. \quad (4)$$

Equation (4) has a square integrable solution  $\psi$  only for a discrete set of positive eigenvalues  $\lambda_0 \geq \lambda_1 \geq \dots > 0$ , with the corresponding real-valued eigenfunctions  $\psi_0, \psi_1, \dots$ .

A discrete version of the eigenproblem (4) is used in [2, eq. (8)] to define the DPSSs. The DPSSs are used to represent the discretized wireless channel taps because these sequences arise in the solution of a discrete spectral concentration problem [2, eq. (5)], and thus form an efficient basis for band-limited channel taps. Similarly, the PSWFs arise as the solutions to the following spectral concentration problem: find a band-limited function with bandwidth  $c > 0$ , whose energy on the interval  $[-1, 1]$ , normalized as a fraction of the total energy, is the highest possible [13]. Specifically, the function  $\psi_0$  maximizes the normalized energy on the interval  $[-1, 1]$ , the function  $\psi_1$  maximizes the normalized energy on the interval  $[-1, 1]$  among the functions orthogonal to  $\psi_0$ , etc.

We consider one OFDM symbol of duration  $KT_s$  (excluding the cyclic prefix), and regard the channel taps as functions defined on the time interval  $[0, KT_s]$ . We model the channel with the maximum Doppler shift of  $\nu_{\max}$  using rescaled PSWFs, whose bandwidth does not exceed  $\nu_{\max}$ . Specifically, we set

$$h_l(t) = \sum_{m=0}^{M-1} b_{lm} \Psi_m(t), \quad t \in [0, KT_s] \quad (5)$$

where  $b_{lm}$  is the  $m$ th PSWF coefficient of the  $l$ th channel tap for  $l = 0, \dots, L-1$ , and

$$\Psi_m(t) = \psi_m \left( \frac{2t}{KT_s} - 1 \right). \quad (6)$$

The bandwidth parameter  $c$  of the PSWFs  $\psi_m$  is set to  $2\nu_{\max}KT_s$ , the latter quantity is known as the time-bandwidth product. In Section IV, we derive explicit formulas for the PSWF-BEM coefficients in terms of the receive signal.

Our reconstruction algorithm requires the evaluation of the Fourier transforms of the PSWFs, which can be expressed in terms of the same PSWFs rescaled by the factor of  $\frac{1}{c}$  [14, eq. (7)]

$$\int_{-1}^1 e^{-j\omega x} \psi_n(x) dx = (-j)^n \sqrt{\frac{2\pi\lambda_n}{c}} \psi_n \left( \frac{\omega}{c} \right), \quad \omega \in \mathbb{R}. \quad (7)$$

A BEM with the Legendre polynomials is introduced in [7]. It is known that the Legendre polynomials are obtained from the PSWFs in the limit as the bandwidth  $c$  decreases to 0 [12, Theorem 5.2]. Consequently, for sufficiently small values of  $c$ , a wireless channel can be reasonably well modeled with the Legendre polynomials; see Section V for simulation results.

#### D. Fourier Coefficients of Channel Taps

An accurate, pilot-aided, FFT-based estimation method for the Fourier coefficients of the channel taps is presented in [7]. With  $L$  discrete channel taps, that method requires  $\mathcal{O}(L \log L)$  flops and  $\mathcal{O}(L)$  memory, and does not require any statistical information. In this paper, we use the same algorithm for estimation of the Fourier coefficients of the channel taps.

We consider the  $l$ th channel tap  $h_l$  on the interval  $[0, KT_s]$ , and define its  $k$ th Fourier coefficient as follows:

$$\mathbf{H}_l[k] = \int_0^{KT_s} e^{-j2\pi k \frac{t}{KT_s}} h_l(t) dt, \quad (8)$$

We assume that estimated Fourier coefficients of the channel tap  $\hat{\mathbf{H}}_l[k]$  are given for  $D^- \leq k \leq D^+$ , where  $D^-$  and  $D^+$  are fixed cutoff frequencies.

Reconstruction of the channel taps from the estimated Fourier coefficients as truncated Fourier series corresponds to the CE-BEM [4]. However, the CE-BEM is not sufficiently accurate for estimation of doubly selective channels because of the Gibbs phenomenon; see [2] and [7]. Nevertheless, estimated Fourier coefficients can be used to estimate the BEM coefficients with respect to a fixed arbitrary basis. In [7], the BEM coefficients are computed by the orthogonal projection of a truncated Fourier series onto the linear space spanned by the basis functions. It is noteworthy, that the projection onto a well chosen basis also remedies the Gibbs phenomenon [15], and results in better approximations for the channel taps. In the next section, we introduce another method for the computation of the BEM coefficients from estimated Fourier coefficients of the channel taps, known as *the inverse reconstruction method*.

### III. INVERSE RECONSTRUCTION METHOD

The objective of the inverse reconstruction method [11] is to reconstruct an unknown function as a linear combination of given basis functions from a finite number of the Fourier coefficients of the function. Specifically, a linear combination is constructed whose Fourier coefficients match the given Fourier coefficients of the unknown function.

Given a function  $f(x)$  defined on the interval  $[-1, 1]$ , and a positive integer  $D$ , we consider the first  $D$  Fourier coefficients of  $f(x)$  given by

$$\hat{f}(d) = \int_{-1}^1 e^{-jd\pi x} f(x) dx, \quad D^- \leq d \leq D^+ \quad (9)$$

where  $D^- = -\lfloor (D-1)/2 \rfloor$ ,  $D^+ = \lfloor D/2 \rfloor$ , and  $\lfloor \cdot \rfloor$  denotes the floor operation. Clearly,  $D^- \leq 0 \leq D^+$ , and  $D^+ - D^- = D - 1$ . We approximately reconstruct the function  $f$  as a linear combination of fixed  $M \leq D$  basis functions  $\Phi_0, \dots, \Phi_{M-1}$

$$f \approx f_M(t) = \sum_{m=0}^{M-1} a_m \Phi_m(t). \quad (10)$$

The essence of the inverse reconstruction method is to require that the  $a_m$ 's minimize the norm of the difference of the  $D$  lowest Fourier coefficients of  $f$  and  $f_M$

$$\left( \sum_{D^- \leq d \leq D^+} |\hat{f}(d) - \hat{f}_M(d)|^2 \right)^{\frac{1}{2}} \quad (11)$$

where  $\hat{f}_M(d)$  is the  $k$ th Fourier coefficient of  $f_M$ . The coefficients  $a_m$  minimizing the expression (11) are computed as the solution of the overdetermined least squares problem

$$\min_{\mathbf{a} \in \mathbb{C}^M} \|\mathcal{P}\mathbf{a} - \hat{\mathbf{f}}\| \quad (12)$$

where  $\mathbf{a} = [a_0, \dots, a_{M-1}]^T$ ,  $\hat{\mathbf{f}} = [\hat{f}(D^-), \dots, \hat{f}(D^+)]^T$ , and  $\mathcal{P}$  is the  $D \times M$  matrix whose entries are the respective Fourier coefficients of the basis functions

$$\mathcal{P}_{dm} = \hat{\Phi}_m(d), \quad (13)$$

$m = 0, \dots, M-1$ ,  $d = D^-, \dots, D^+$ . If  $\mathcal{P}$  has full rank, then the overdetermined least squares problem (12) has a unique solution given by:

$$\mathbf{a} = \mathcal{P}^\dagger \hat{\mathbf{f}} \quad (14)$$

where  $\mathcal{P}^\dagger$  is the Moore–Penrose pseudoinverse of the matrix  $\mathcal{P}$ .

We note that the inverse reconstruction method can be used to compute approximate expansion coefficients of a function with respect to an arbitrary basis from the Fourier coefficients of the function. Depending on the choice of the basis, the Fourier coefficients appearing in the (13) may be known in a closed form, or may need to be precomputed by a suitable numerical integration method.

One of the main motivations behind the development of this method is to mitigate the Gibbs phenomenon [11], [16]. Typically, orthogonal analytic functions, e.g., polynomials, are used for reconstruction if the unknown function is additionally assumed to be analytic.

### IV. ESTIMATION OF BEM COEFFICIENTS

#### A. Overview

We apply the theory developed in the previous section to compute the PSWF expansion coefficients by the inverse method. Given a positive integer  $D$ , we estimate the first  $D$  Fourier coefficients of the channel

TABLE I  
OPERATION COUNT FOR THE PROPOSED ALGORITHM PER OFDM SYMBOL OBTAINED FOR  $K = 256, L = 32, D = 3,$  AND  $M = 2$  (AS USED IN THE SIMULATIONS)

step	description	operations	example
1	computation of Fourier coefficients [7]	$DL \log L + DL$	576
2	computation of BEM coefficients	$MDL$	192

taps  $\tilde{\mathbf{H}}_l[d]$  using the pilot assisted algorithm described in [7]. We consider the channel taps on the interval  $[0, KT_s]$ , and approximate them using the rescaled PSWFs  $\Psi_m$  defined by (6). A straightforward calculation shows that the Fourier coefficients  $\hat{\Psi}_m(d)$  are related to those of the PSWFs as follows:

$$\hat{\Psi}_m(d) = (-1)^d \frac{KT_s}{2} \hat{\psi}_m(d). \quad (15)$$

Using (7), we obtain

$$\hat{\Psi}_m(d) = (-1)^d (-j)^m KT_s \sqrt{\frac{\pi \lambda_m}{2c}} \psi_m\left(\frac{d\pi}{c}\right) \quad (16)$$

where  $c = 2\nu_{\max}KT_s$  as explained in Section II. In view of (14), the estimated PSWF coefficients of the  $l$ th channel tap are given by

$$[\tilde{b}_{l,0}, \dots, \tilde{b}_{l,M-1}]^t = \mathcal{P}^\dagger [\tilde{\mathbf{H}}_l[D^-], \dots, \tilde{\mathbf{H}}_l[D^+]]^t \quad (17)$$

where  $\mathcal{P}$  is defined by (13).

The estimated PSWF expansion coefficients can be used for equalization of the received signal without creating the entire channel matrix, see [8]. We note that the proposed BEM estimation method can be used with any set of basis functions, we use the PSWFs only for illustration.

### B. Detailed Description and Complexity Analysis

We assume that the pseudoinverse of the matrix  $\mathcal{P}$ , which we denote by  $\mathcal{P}^\dagger$ , is precomputed. The matrix  $\mathcal{P}^\dagger$  is dimensioned  $M \times D$ , and thus requires  $MD$  real numbers for its storage. The first  $D$  Fourier coefficients for all  $L$  channel taps, i.e.,  $\tilde{\mathbf{H}}_l[d]$ , are computed as described in [7]. That method requires exactly  $DL \log L + DL$  complex flops, and the storage of  $DL + L$  complex numbers. Finally, the PSWF expansion coefficients of the channel taps are computed using (17). This step requires  $MDL$  flops, and the storage of  $ML$  complex numbers. The steps of the algorithm are presented in Table I, together with their complexity, and a typical number of operations per OFDM symbol for a setup with  $K = 256$  subcarriers and  $L = K/8$  discrete path delays.

### C. Comparison With the Previous Method

In the Appendix, we show that the proposed estimation algorithm is algebraically equivalent to the method proposed in [3]. In that paper, the parameter  $B_c$  denotes the bandwidth of the approximating frequency domain channel matrix, and  $Q$  denotes the order of the BEM basis. These two parameters in [3] are related to the parameters  $D$  and  $M$ , respectively, of the present paper. Specifically,  $M = Q + 1$  and  $D = 2B_c + 1$ . However, the proposed method has dramatically lower complexity than that of [3]. Specifically, with  $L$  channel taps, the proposed method requires  $\mathcal{O}(L \log L)$  operations and  $\mathcal{O}(L)$  memory, whereas the least square method in [3] requires  $\mathcal{O}(L^2)$  of both flops and memory. The improvement complexity from  $\mathcal{O}(L^2)$  to  $\mathcal{O}(L \log L)$  is significant. For example, Mobile WiMAX with  $K = 2048$  subcarriers exhibits a typical discrete path delay of  $L = \frac{K}{8} = 256$ ; see [1]. In this case, the proposed algorithm is faster by a factor of  $\frac{L}{\log L} = 32$ .

TABLE II  
SIMULATION PARAMETERS: (a) TRANSMISSION SIMULATION PARAMETERS AND (b) CHANNEL SIMULATION PARAMETERS

(a)	
number of subcarriers ( $K$ )	256
intercarrier spacing ( $f_s$ )	10.9 kHz
bandwidth ( $B = Kf_s$ )	2.8 MHz
sampling time ( $T_s = 1/B$ )	0.357 $\mu$ s
cyclic prefix ( $L_{cp} = K/8$ )	32
symbol duration ( $(K + L_{cp})T_s$ )	102.9 $\mu$ s
carrier frequency ( $f_c$ )	5.8GHz
error correcting code	1/2-conv.
constellation	4QAM
(b)	
max. path delay	11.4 $\mu$ s
max. Doppler shift	16% $f_s, 62\% f_s$
average path gain	-2 dB
fading	Rayleigh
Doppler spectrum	Jakes
$E_b/N_0$	5 - 30 dB

## V. COMPUTER SIMULATIONS

### A. Description of Experiments

The OFDM transmission, and the wide sense stationary uncorrelated scattering (WSSUS) channel are simulated using parameters given in Table II. At the receiver's end, we process one OFDM symbol at a time. We first discard the cyclic prefix from the receive signal. Next we estimate the BEM coefficients, using the BEM with the PSWFs and the BEM with the Legendre polynomials. For estimating the BEM coefficients from the estimated Fourier coefficients, we use the inverse method proposed in this paper, and the orthogonal projection method proposed in [7]. The estimated BEM coefficients are further used for equalization of the receive signal; see [8]. As a measure of performance, we report the normalized mean-square error (NMSE) of the channel taps, averaged over 100 000 OFDM symbols. Furthermore, we also report the BER averaged over 100 000 OFDM symbols, computed after equalization, discarding pilots, quantization, deinterleaving, and decoding using the BCJR algorithm, which is named after its inventors: Bahl, Cocke, Jelinek and Raviv. We note that reconstruction of the channel matrix is not necessary for equalization [8].

### B. Discussion of Simulation Results

Fig. 1(a) and (b) shows the NMSE as a function of  $E_b/N_0$  for the BEM with the Legendre polynomials and the PSWFs, respectively. Similarly, Fig. 2(a) and (b) shows the BER after equalization as a function of  $E_b/N_0$  for the BEM with the Legendre polynomials and the PSWFs, respectively. A channel with the Doppler spread of 16% of the intercarrier frequency is used in the above experiments. For both bases, i.e., the PSWFs and the Legendre polynomials, we compute  $D = 3$  Fourier coefficients per channel tap, and use the BEM model order  $M = 2$ . In all figures, the curve labeled "conventional" is obtained

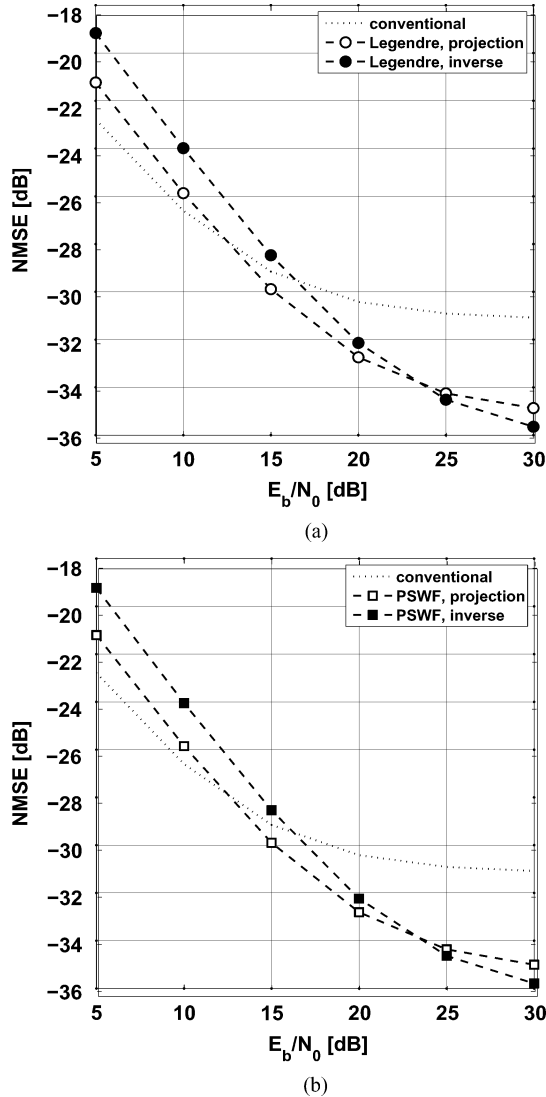


Fig. 1. NMSE versus  $E_b/N_0$  at a Doppler of spread 16% of intercarrier frequency spacing. (a) BEM with Legendre polynomials. (b) BEM with PSWFs.

via single tap estimation in the frequency domain. From these figures, it is evident that the quality of estimation with the PSWFs and the Legendre polynomials is equal at relatively low Doppler spreads. We also note that estimation with the projection method is more robust to ambient noise than the estimation with the inverse method.

Fig. 3(a) and (b) shows the NMSE and the BER as functions of  $E_b/N_0$  with a channel having a Doppler spread of 62% of the intercarrier frequency spacing. We notice that at such a high Doppler spread, estimation with the PSWFs with a proper time-bandwidth product is significantly more accurate than one with the Legendre polynomials. For the BEM with the PSWFs, the inverse method and the projection method work equally well. On the other hand, for the BEM with the Legendre polynomials, the inverse method has significantly better BERs than the projection method. The performance of the BEM with the PSWFs depends on a proper choice of the time-bandwidth product for the PSWFs (see [3] for a discussion), whereas the BEM with the Legendre polynomials does not have such a parameter.

## VI. CONCLUSION

We present a novel algorithm for estimation of the BEM coefficients in OFDM systems. The proposed method efficiently computes

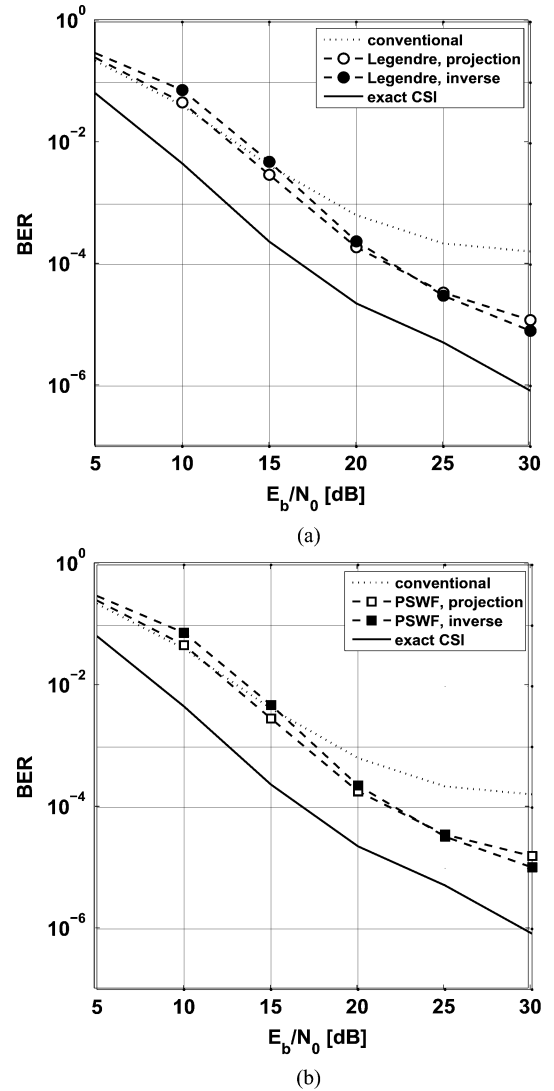


Fig. 2. BER versus  $E_b/N_0$  at a Doppler of spread 16% of intercarrier frequency spacing. (a) BEM with Legendre polynomials. (b) BEM with PSWFs.

the BEM coefficients of the channel taps from their estimated Fourier coefficients. We employ the inverse reconstruction method for this purpose. We compare the proposed method with an older one, which uses the orthogonal projection for the same purpose. We observe in our numerical simulations that the projection method works better for low to medium Doppler shifts, and the inverse reconstruction method works better for relatively high Doppler shifts.

With  $L$  discrete channel taps, the proposed BEM coefficient estimation method requires  $\mathcal{O}(L \log L)$  flops and  $\mathcal{O}(L)$  memory. By contrast, a previous method by Tang *et al.* requires  $\mathcal{O}(L^2)$  flops and memory. The estimated BEM coefficients can be used directly for equalization, without constructing the channel matrix; see [8]. In addition, we propose the prolate spheroidal wave functions (PSWFs) as a basis for the channel taps.

## APPENDIX A

### RELATIONSHIP TO PREVIOUS ESTIMATION METHODS

In this Appendix, we describe how our method is related to that of Tang *et al.* [3]. The entries of the time domain channel matrix  $H$  are zero, except possibly for the entries of the form  $H(n, n-l) = h_l[n]$ ,

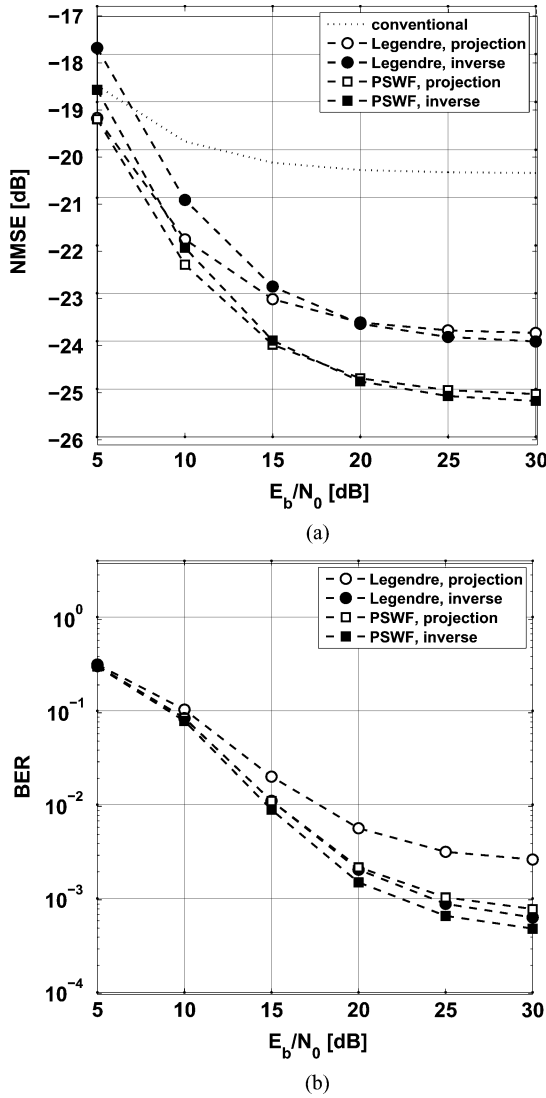


Fig. 3. Doppler of spread 62% of intercarrier frequency spacing. (a) NMSE versus  $E_b/N_0$ . (b) BER versus  $E_b/N_0$ .

$l = 0, \dots, L - 1$ . In the following, we express the entries of the frequency domain channel matrix  $H_F$  in terms of the BEM coefficients of the time domain channel matrix  $H$ .

$$\begin{aligned}
 H_F(k, k+d) &= \frac{1}{K} \sum_{0 \leq r, s < K} e^{-j2\pi \frac{kr}{K}} H(r, s) e^{j2\pi \frac{s(k+d)}{K}} \\
 &= \frac{1}{K} \sum_{l=0}^{L-1} \sum_{n=0}^{K-1} e^{-j2\pi \frac{kn}{K}} h_l[n] e^{j2\pi \frac{(n-l)(k+d)}{K}} \\
 &= \frac{1}{K} \sum_{l=0}^{L-1} \sum_{n=0}^{K-1} e^{-j2\pi \frac{kn}{K}} \left( \sum_{m=0}^{M-1} b_{lm} B_m[n] \right) e^{j2\pi \frac{(n-l)(k+d)}{K}} \\
 &= \sum_{l=0}^{L-1} e^{-j2\pi \frac{l(k+d)}{K}} \sum_{m=0}^{M-1} b_{lm} \frac{1}{K} \sum_{n=0}^{K-1} e^{j2\pi \frac{nd}{K}} B_m[n] \\
 &= \sum_{l=0}^{L-1} e^{-j2\pi \frac{l(k+d)}{K}} \sum_{m=0}^{M-1} b_{lm} \hat{B}_m(-d) \\
 &= \sum_{m=0}^{M-1} \hat{B}_m(-d) \sum_{l=0}^{L-1} e^{-j2\pi \frac{l(k+d)}{K}} b_{lm}
 \end{aligned} \tag{18}$$

$$\begin{aligned}
 &= \sum_{m=0}^{M-1} \hat{B}_m(-d) \sum_{l=0}^{L-1} e^{-j2\pi \frac{l(k+d)}{K}} b_{lm} \\
 &= \sum_{m=0}^{M-1} \hat{B}_m(-d) \sum_{l=0}^{L-1} e^{-j2\pi \frac{l(k+d)}{K}} b_{lm}
 \end{aligned} \tag{19}$$

where  $\hat{B}_m(d)$  denotes the  $d$ th Fourier coefficient of the  $m$ th basis function.

The approach of [3], and also of this paper, is to form a set of equations with the entries of  $H_F$  corresponding to the pilot locations, and solve it for the BEM coefficients  $b_{lm}$ . We observe that using (19) is equivalent to (12) in [3]. The complexity of this approach is  $O(L^2)$ . Our approach is based on (18), and with our frequency-domain Kronecker Delta (FDKD) pilot arrangement, (18) gives rise to a factorization of the system matrix into the DFT matrix of order  $L$ , and a  $D \times M$  matrix  $\mathcal{P}$ . Consequently, the complexity of our approach is  $O(L \log L)$ .

#### ACKNOWLEDGMENT

The authors are very grateful to the referees for their detailed comments and suggestions which have improved this paper.

#### REFERENCES

- [1] *Draft IEEE Standard for Local and Metropolitan Area Networks Part 16: Air Interface for Fixed and Mobile Broadband Wireless Access Systems*, IEEE Draft Standard 802.16e/D7, 2005.
- [2] T. Zemen and C. F. Mecklenbrauker, "Time-variant channel estimation using discrete prolate spheroidal sequences," *IEEE Trans. Signal Process.*, vol. 53, no. 9, pp. 3597–3607, Sep. 2005.
- [3] Z. Tang, R. C. Cannizzaro, G. Leus, and P. Banelli, "Pilot-assisted time-varying channel estimation for OFDM systems," *IEEE Trans. Signal Process.*, vol. 55, no. 5, pp. 2226–2238, May 2007.
- [4] H. A. Cirpan and M. K. Tsatsanis, "Maximum likelihood blind channel estimation in the presence of Doppler shifts," *IEEE Trans. Signal Process.*, vol. 47, no. 6, pp. 1559–1569, Jun. 1999.
- [5] G. Leus, "On the estimation of rapidly varying channels," in *Proc. Eur. Signal Process. Conf. (EUSIPCO)*, Sep. 2004, vol. 4, pp. 2227–2230.
- [6] D. K. Borah and B. T. Hart, "Frequency-selective fading channel estimation with a polynomial time-varying channel model," *IEEE Trans. Commun.*, vol. 47, no. 6, pp. 862–873, Jun. 1999.
- [7] T. Hrycak, S. Das, G. Matz, and H. Feichtinger, "Practical estimation of rapidly varying channels for OFDM systems," *IEEE Trans. Commun.*, vol. 59, no. 11, pp. 3040–3048, 2011.
- [8] T. Hrycak, S. Das, G. Matz, and H. G. Feichtinger, "Low complexity equalization for doubly selective channels modeled by a basis expansion," *IEEE Trans. Signal Process.*, vol. 58, no. 11, pp. 5706–5719, Nov. 2010.
- [9] K. Fang, L. Rugini, and G. Leus, "Low-complexity block turbo equalization for OFDM systems in time-varying channels," *IEEE Trans. Signal Process.*, vol. 56, no. 11, pp. 5555–5566, Nov. 2008.
- [10] P. Schniter, "Low-complexity equalization of OFDM in doubly selective channels," *IEEE Trans. Signal Process.*, vol. 52, no. 4, pp. 1002–1011, Apr. 2004.
- [11] B. D. Shizgal and J.-H. Jung, "Towards the resolution of the Gibbs phenomena," *J. Comput. Appl. Math.*, vol. 161, no. 1, pp. 41–65, 2003.
- [12] J. P. Boyd, "Prolate spheroidal wavefunctions as an alternative to Chebyshev and Legendre polynomials for spectral element and pseudospectral algorithms," *J. Comput. Phys.*, vol. 199, no. 2, pp. 688–716, Nov. 2004.
- [13] D. Slepian, "Some comments on Fourier analysis, uncertainty and modelling," *SIAM Rev.*, vol. 25, no. 3, pp. 379–393, 1983.
- [14] I. C. Moore and M. Cada, "Prolate spheroidal wave functions, an introduction to the Slepian series and its properties," *Appl. Comput. Harmon. Anal.*, vol. 16, pp. 208–230, 2004.
- [15] D. Gottlieb and C.-W. Shu, "On the Gibbs phenomenon and its resolution," *SIAM Rev.*, vol. 39, no. 4, pp. 644–668, 2003.
- [16] T. Hrycak and K. Gröchenig, "Pseudospectral Fourier reconstruction with the modified inverse polynomial reconstruction method," *J. Comput. Phys.*, vol. 229, pp. 933–946, Feb. 2010.